scientific reports

Check for updates

OPEN

Ultrafast switching in synthetic antiferromagnet with bilayer rare-earth transition-metal ferrimagnets

Chung Ting Ma[1]✉, Wei Zhou[1] & S. Joseph Poon[1,2]

In spintronics, it is important to be able to manipulate magnetization rapidly and reliably. Several methods can control magnetization, such as by applying current pulses or magnetic fields. An applied current can reverse magnetization with nanosecond speed through the spin torque effect. For faster switching, subpicosecond switching with femtoseconds laser pulse has been achieved in amorphous rare-earth transition-metal ferrimagnets. In this study, we employed atomistic simulations to investigate ultrafast switching in a synthetic antiferromagnet with bilayer amorphous FeGd ferrimagnets. Using a two-temperature model, we demonstrated ultrafast switching in this synthetic antiferromagnet without external magnetic fields. Furthermore, we showed that if we initially stabilize a skyrmion in this heterostructure, the ultrafast laser can switch the skyrmion state using the same mechanism. Furthermore, this bilayer design allows the control of each ferrimagnetic layer individually and opens the possibility for a magnetic tunnel junction.

The ability to control magnetization is a critical component of designing memory and logical devices. In thin films, magnetizations are commonly manipulated through current or external fields. In spintronic devices, currents are often used to induce spin-transfer torque and spin-orbit torque to reliably switch magnetizations without magnetic fields[1–5]. Besides electrical current, a laser pulse can also induce changes in magnetization. Subpicosecond demagnetization with femtosecond laser pulse was first observed in ferromagnetic nickel film[6]. Since then, ultrafast manipulation of magnetization has drawn considerable interest for its potential applications. In ferromagnets, a multistep procedure has been demonstrated to switch magnetization[7–10]. For example, in FePt nanoparticles, magnetizations are first thermally demagnetized, then re-magnetized through the laser-induced inverse Faraday effect[9]. In antiferromagnets, optical switching of antiferromagnetic order is observed in multiferroic $TbMnO_3$ at 18 K[11]. Furthermore, reliable all-optical switching of magnetization in easy-plane CrPt has been proposed by utilizing the inverse Faraday effect[12]. Nonetheless, one-shot all-optical subpicosecond switching has only been observed in ferrimagnets, such as rare-earth transition metal (RE-TM) ferrimagnets[13–20] and recently, Mn-based crystalline alloys[21].

Amorphous RE-TM ferrimagnetic films are one of the more appealing materials for applications. They consist of two antiferromagnetically coupled RE-TM sublattices, which align in an antiparallel direction. There exists a compensation temperature (T_{Comp}) where the magnetic moments of the two sublattices cancel each other and magnetization goes to zero[22,23]. RE-TM films contain several attractive properties, including perpendicular magnetic anisotropy (PMA)[24,25] and high domain wall velocity[26,27]. Furthermore, they are deposited at room temperature[28] and their composition can be tuned to adjust magnetization and coercivity[23,28]. Recent experiments also observed skyrmions in RE-TM thin films[27,29–31]. One of the most intriguing properties of RE-TM ferrimagnet is the access to one-shot all-optical ultrafast switching[13–20]. In previous studies, it is revealed that angular momentum exchange between the two different sublattices is a key ingredient in all-optical switching[15,32,33]. The requirement of having two different sublattices makes ferrimagnets, such as RE-TM, one of the few PMA materials to have this capability.

In this study, we investigate laser-induced ultrafast switching in a synthetic antiferromagnet (SAF) formed from a bilayer RE-TM ferrimagnet . A schematic diagram of this heterostructure is shown in Fig. 1. In this heterostructure, two different compositions of 5 nm thick FeGd combine to form a 10 nm thick SAF, with one layer having T_{Comp} above room temperature and the other having T_{Comp} below room temperature. Such control of

[1]Department of Physics, University of Virginia, Charlottesville, Virginia 22904, USA. [2]Department of Materials Science and Engineering, University of Virginia, Charlottesville, Virginia 22904, USA. ✉email: ctm7sf@virginia.edu

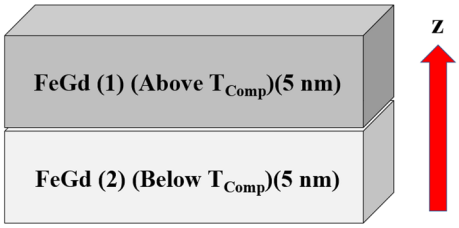

Figure 1. A schematic diagram of a synthetic antiferromagnet used in this study. Two 5 nm thick FeGd combines to form the synthetic antiferromagnet. In this study, layer 1 has T_{Comp} at 350 K, above room temperature, and layer 2 has T_{Comp} at 250 K, below room temperature. The z-direction in this study is defined as the out-of-plane direction.

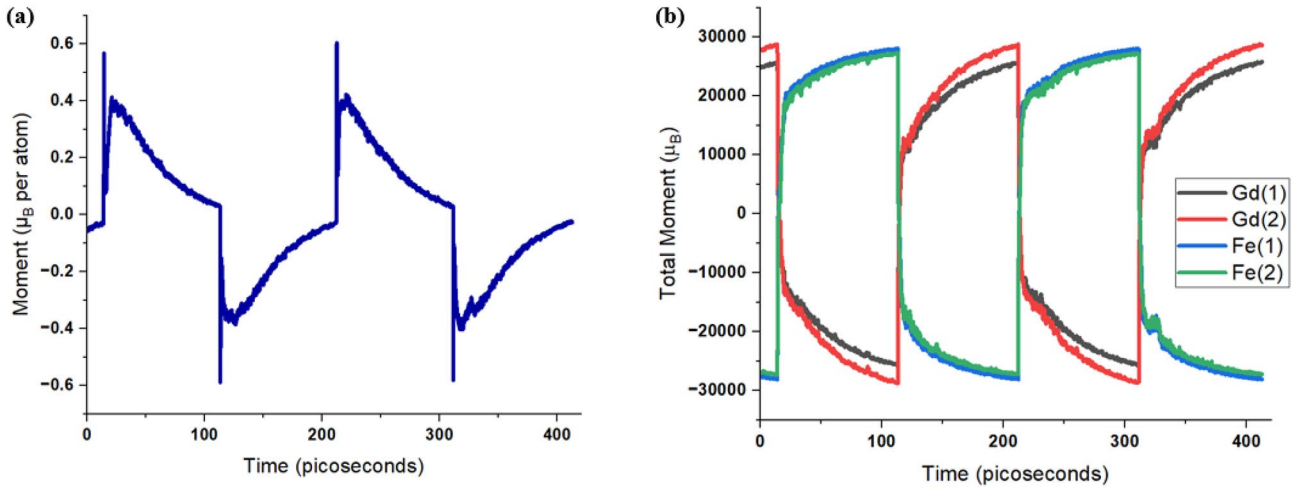

Figure 2. (**a**) Time evolution of magnetic moment per atom with application of a 100-fs laser pulse with 30 J/m^2 fluence every 100 ps. (**b**) Time evolution of total magnetic moment of Gd and Fe sublattice in each FeGd layer with application of a laser pulse every 100 ps.

T_{Comp} in RE/TM films has been achieved experimentally by tuning composition of Fe and Gd[23], where a higher T_{Comp} was achieved by increasing rare-earth concentration. To elaborate, this SAF arises from the cancellation of magnetization between the top and bottom FeGd layer. The magnetization in each layer is designed to be opposite but equal in magnitude at room temperature. This is obtained by choosing the T_{Comp} of the top layer to be 350 K and the T_{Comp} of the top layer to be 250 K. This heterostructure presents several advantages. Compared to SAF with ferromagnet or multilayer RE/TM films, SAF with RE-TM allows more flexible tuning of each layer. The thickness[34,35] and composition[23] of each layer can be varied while the net magnetization stays zero, and PMA remains robust. In contrast, SAF with ferromagnet and multilayer RE-TM films are limited in thickness and composition to maintain PMA[18,36]. Furthermore, the use of thicker layers diminishes the relative strength of interface exchange on an individual layer. This opens the possibility of switching each layer individually. In this study, we explored laser-induced ultrafast switching in SAF with RE-TM by using a two-temperature model for laser irradiation[37,38]. We found deterministic spins switching in this heterostructure, like those observed in single-layer RE-TM films. More importantly, synchronized switching are found within the same sublattice in the FeGd bilayer. Furthermore, we stabilized skyrmions in this heterostructure as initial states and found switching remains robust with a laser pulse. These findings pave the way to employ SAF with a bilayer RE-TM for spintronics applications.

Results and disscussions

Figure 2 shows the results of ultrafast switching in SAF with FeGd after laser pulses. Initially, the spins of Fe sublattices are pointing down (- z-direction) and the spins of Gd sublattices are pointing up (+ z-direction). The spins are initialized by the application of a 0.01 T out-of-plane magnetic field, and no external fields are applied after initialization and during the application of laser pulses. This is a stable configuration in this heterostructure as the exchange couplings between the two FeGd layers align the spins within the same sublattice parallel and the spins in different sublattices antiparallel. Also, magnetic anisotropy in FeGd holds the magnetic moment in an out-of-plane direction without an external field. After the application of a 100-fs laser pulse with 30 J/m^2 fluence, the magnetic moments in both sublattices reverse. As shown in Fig. 2b, spins in Gd sublattices reverse from the positive to the negative direction, and spins in Fe sublattices reverse from the negative to the positive direction. Furthermore, Gd spins in both layer 1 and layer 2 reverse simultaneously and the same switching is observed in

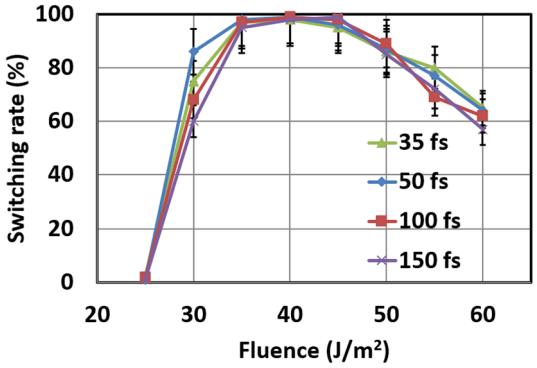

Figure 3. Switching rate of magnetization in synthetic antiferromagnet with bilayer FeGd as a function of laser fluence. Simulations at each fluence is repeated 128 times and the switching rate is the percentage of switching occurred out of 128 simulations. Error bars correspond to one standard deviation from avenging. 35 fs (green), 50 fs (blue), 100 fs (red) , and 150 fs (purple) shows similar switching rate.

Fe spins of both layers. From Fig. 2a, the total moment deviates from zero after the excitation by a laser pulse. This is due to the different exchange couplings and relaxation time of Fe and Gd sublattices. As discussed by previous publications[14–16], RE and TM sublattice have different relaxation times and lead to a transient state, where spins in RE and TM align in parallel after the first few picoseconds of a laser pulse. In this SAF, within picoseconds the initial spike in magnetic moment corresponds to the transient state, matching the previous study of single-layer RE-TM films. After the initial spike, a large downward spike is observed. This is the consequence of the high temperature from the laser pulse. As a result, the magnetic moments are not synchronized in one direction and lead to a smaller total moment. Then, as the temperature cools down, the spins in Fe sublattice, which has stronger coupling, become more aligned, which leads to an increase in the total moment. As the temperature cools down further, the magnetic moment begins to decrease. This is explained by the gradual alignment of the Gd sublattice over this period, which points opposite to the Fe atoms, and the spins begin to relax back to one of the ferrimagnetic ground states. After 100 ps, the total magnetic moment approaches back to zero. From Fig. 2b, the moments of each sublattice are now pointing in opposite directions, corresponding to opposite spin directions from the initial configuration. Subsequence laser pulses, which were applied every 100 ps, show deterministic switching of spins in this heterostructure.

To validate the repeatability of this switching, we repeated the simulations with various laser fluence and laser pulse width. Figure 3 shows the switching rate of spins in SAF with FeGd with laser fluence from 25 J/m^2 to 60 J/ m^2 and laser pulse widths of 35 fs, 50 fs, 100 fs, and 150 fs. The simulations have repeated 128 times for each set of fluence and laser pulse width, and the switching rate is the percentage of switching observations out of 128 simulations. From Fig. 3, the switching rate is similar in all four laser pulse width (35 fs, 50 fs, 100 fs, and 150 fs) for various fluences. On the other hand, varying laser fluence has a significant impact on the switching rate. With a laser fluence of 25 J/ m^2, the switching rate is near zero. As the laser fluence increases to 30 J/ m^2, the switching rate increases to about 70 %. Between laser fluence of 35–45 J/ m^2, the switching rate is above 90 %. Above 45 J/ m^2, switching decreases with increases in laser fluence, reducing to about 60 % at a laser fluence of 60 J/ m^2. While the mechanisms behind this dependence remain unknown, this phenomenon is likely related to the angular momentum exchange between the Fe and Gd sublattices. As discussed in other publications[15,33,34], angular momentum exchange between the two different sublattices is a crucial component of all-optical switching in RE-TM films. From intuition, at low laser fluence ($<$ 25 J/ m^2), there is not enough energy to initiate the exchange of angular momentum, resulting in a zero switching rate. For high laser fluence ($>$ 45 J/ m^2), an excess temperature may lead to excessive fluctuations in spins and reduces the effectiveness of angular momentum exchange between the two sublattices.While the temperature differences for different fluences certainly play a role in the switching rate, they also affect the angular momentum exchange between the two sublattices in the switching process. Further investigations are needed to reveal the underlying reasons, which are beyond the scope of this study.

We further investigate the potential of using ultrafast switching in other magnetic states in RE-TM ferrimagnets. Figure 4 shows the ultrafast switching of a 20 nm skyrmion in SAF with FeGd. This skyrmion was initially stabilized through the interfacial Dzyaloshinskii-Moriya interaction[39,40] under 0.01 T. Details of this skyrmion calculation were discussed in previous publications[41]. As seen in Fig. 4b, initially, the spins of Fe and Gd sublattices form a skyrmion. In Fe sublattice, the spins in the core of a skyrmion are pointing in the positive direction and the spins outside are pointing in the negative direction. The spins in Gd sublattice align antiparallel to the spins in Fe sublattice. After applying a 100 fs laser pulse with 30 J/m^2 fluence, the spins in the heterostructures reverse from the initial configuration. As the spins relax, they relax back to a skyrmion configuration with spins opposite to the initial configuration, as illustrated in Fig. 4b. From Fig. 4a, subsequence laser pulses show the spin reversal process is repeatable. This reversal of spin texture likely arises from the angular momentum exchange between the two different sublattices, which leads to maintaining spin texture in a subpicosecond timescale. This result demonstrates another unique feature of all-optical switching in RE-TM ferrimagnet. Furthermore, this bilayer design opens up the possibility to incorporate into a magnetic tunnel junction. One can introduce

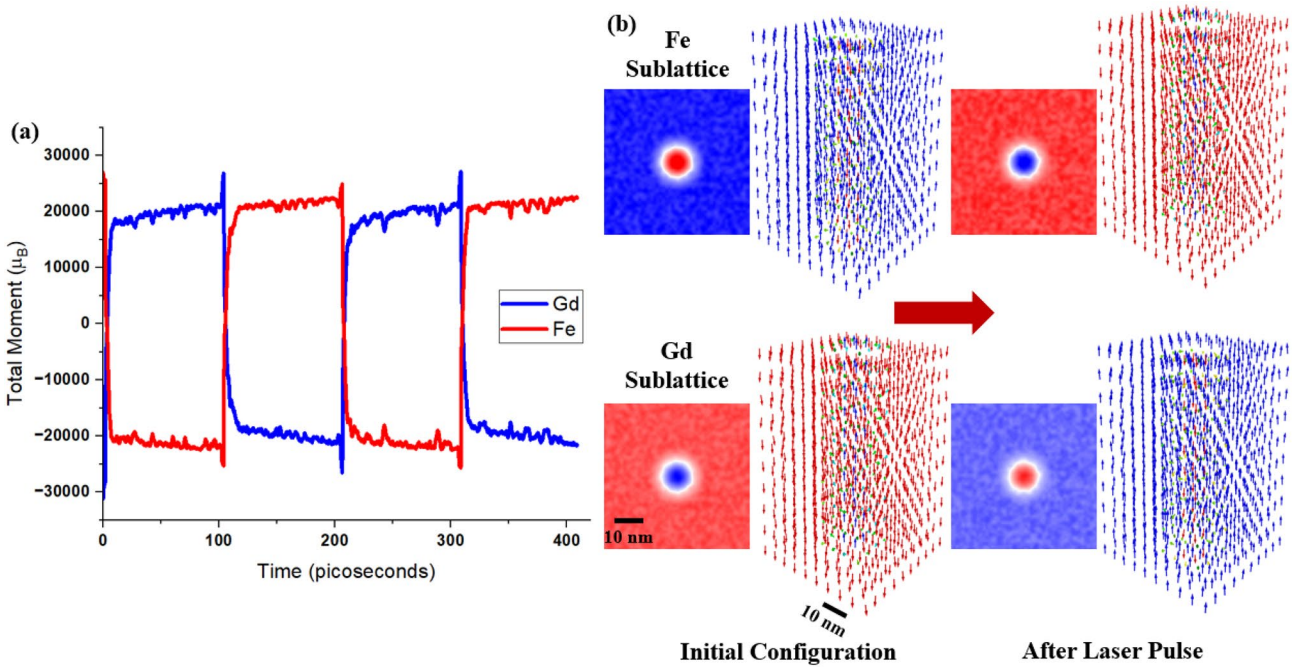

Figure 4. Ultrafast switching of a skyrmion in a synthetic antiferromagnet with bilayer FeGd. (**a**) Time evolution of magnetic moment after application of a 100-fs laser pulse with 30 J/m^2 fluence. (**b**) Schematic representation of spins in Fe and Gd sublattice before and after switching by laser pulse. Inserted figures indicate the top-view of the color mapping of out-of-plane reduced magnetic moments (m_z) in both Fe and Gd sublattices, before and after switching by laser pulse. Red colors represent down magnetic moments, blue colors represents up magnetic moments, and white colors represent in-plane magnetic moments. Both layer of FeGd are shown here, where the top half of each schematic correponds to the top FeGd layer and the bottom half corresponds to the bottom FeGd layer.

exchange bias by adding an antiferromagnetic layer on top of the top FeGd layer. By doing so, the exchange bias effect from the antiferromagnetic layer can enhance or reduce the barrier of switching in the top FeGd layer, which results in parallel or anti-parallel spins in each sublattice between the top and bottom FeGd layer. Of course, such heterostructure will need to be tested and optimized experimentally.

Conclusions

We have performed atomistic simulations to study all-optical ultrafast switching in a 10-nm thick synthetic antiferromagnet with bilayer amorphous rare-earth transition-metal ferrimagnet. Through this study, we confirmed deterministic spin switching in the synthetic antiferromagnet by a femtosecond laser pulse. Furthermore, we demonstrated the reversal of magnetization in a skyrmion using a laser pulse. These results indicate promise in the applications of synthetic antiferromagnet with ferrimagnetic heterostructures in future energy-efficient high-density spintronic devices.

Methods

We built an atomistic model of Fe and Gd atoms on the FCC lattice with in-plane periodic boundary conditions. The Fe and Gd atoms are randomly distributed in the FCC lattice. For a 10 nm thick SAF, this model contains 32 x 32 x 32 sites, with half the sites (32 x 32 x 16) belonging to each layer of 5 nm thick RE-TM in the SAF. A semi-classical two-temperature model is employed to calculate the temporal evolution of electron and lattice temperature under the application of femtosecond laser irradiation[37,38]. Figure 5 shows the temperature profile of a 100 fs laser pulse with 30 J/m^2 fluence. Within 0.1 ps, the electronic temperature reaches a peak of over 1300 K, and the lattice temperature reaches just below 600 K. Both temperatures are above the measured Curie temperature of 540 K[42]. The atomistic spins are coupled to the electron temperature in the two-temperature model[37,38]. A stochastic Landau-Lifshitz-Gilbert (LLG) equation is used to model the magnetization dynamics[43]. Table 1 summarizes the parameters used for modeling magnetization dynamics, which were obtained from Ostler et al. and Radu et al.[14,42]. The anisotropy (K_u) is along the z-direction. The Dzyaloshinskii-Moriya interaction (DMI) follows an exponential decay, with the DMI decays from the bottom interface[41]. The strength of the interfacial DMI is 1.2 mJ/m^2. Initially, we applied an out-of-plane magnetic field to align the spins in both sublattices in the out-of-plane direction, with the Gd sublattice pointing parallel to the + z direction. To create the initial state with skyrmion, a 0.01 T magnetic field is applied[41]. After initialization, the magnetic field is set to zero throughout the calculation.

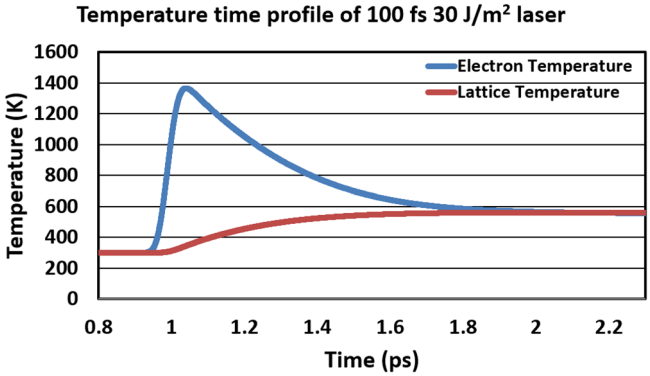

Figure 5. Temporal evolution of electron and lattice temperature after irradiation of a 100-fs laser pulse with 30 J/m^2 fluence.

Parameter	Value
Fe Magnetic moment (μ_{Fe})	2.22 μ_B
Gd Magnetic moment (μ_{Gd})	7.60 μ_B
Fe-Fe Exchange Interaction (J_{Fe-Fe})	2.83 x 10^{-21} J
Gd-Gd Exchange Interaction (J_{Gd-Gd})	1.26 x 10^{-21} J
Fe-Gd Exchange Interaction (J_{Fe-Gd})	−1.09 x 10^{-21} J
Anisotropy (K_u)	0.30 x 10^{-5} J/m^3
Damping (α)	0.05
Fe Gyromagnetic ratio (γ_{Fe})	1.85 $T^{-1}s^{-1}$
Gd Gyromagnetic ratio (γ_{Gd})	1.76 $T^{-1}s^{-1}$

Table 1. Parameters used for modeling magnetization dynamics in FeGd, which were obtained from Ostler el al. and Radu et al.[14,42].

Data availability

The datasets generated during and/or analyzed during the current study are available from the corresponding author on reasonable request.

Received: 8 August 2022; Accepted: 11 November 2022
Published online: 19 November 2022

References

1. Diao, Z. *et al.* Spin-transfer torque switching in magnetic tunnel junctions and spin-transfer torque random access memory. *J. Phys. Condens. Matter* **19**, 165209. https://doi.org/10.1088/0953-8984/19/16/165209 (2007).
2. Manchon, A. *et al.* Current-induced spin-orbit torques in ferromagnetic and antiferromagnetic systems. *Rev. Mod. Phys.* **91**, 035004. https://doi.org/10.1103/RevModPhys.91.035004 (2019).
3. Grimaldi, E. *et al.* Single-shot dynamics of spin-orbit torque and spin transfer torque switching in three-terminal magnetic tunnel junctions. *Nat. Nanotechnol.* **15**, 111–117. https://doi.org/10.1038/s41565-019-0607-7 (2020).
4. DuttaGupta, S. *et al.* Spin-orbit torque switching of an antiferromagnetic metallic heterostructure. *Nat. Commun.* **11**, 5715. https://doi.org/10.1038/s41467-020-19511-4 (2020).
5. Liu, L. *et al.* Symmetry-dependent field-free switching of perpendicular magnetization. *Nat. Nanotechnol.* **16**, 277–282. https://doi.org/10.1038/s41565-020-00826-8 (2021).
6. Beaurepaire, E., Merle, J.-C., Daunois, A. & Bigot, J.-Y. Ultrafast spin dynamics in ferromagnetic nickel. *Phys. Rev. Lett.* **76**, 4250–4253. https://doi.org/10.1103/PhysRevLett.76.4250 (1996).
7. Lambert, C.-H. *et al.* All-optical control of ferromagnetic thin films and nanostructures. *Science* **345**, 1337–1340. https://doi.org/10.1126/science.1253493 (2014).
8. Medapalli, R. *et al.* Multiscale dynamics of helicity-dependent all-optical magnetization reversal in ferromagnetic Co/Pt multilayers. *Phys. Rev. B* **96**, 224421. https://doi.org/10.1103/PhysRevB.96.224421 (2017).
9. John, R. *et al.* Magnetisation switching of FePt nanoparticle recording medium by femtosecond laser pulses. *Sci. Rep.* **7**, 4114. https://doi.org/10.1038/s41598-017-04167-w (2017).
10. Hamamera, H., Guimarães, F. S. M., dos Santos Dias, M. & Lounis, S. Polarisation-dependent single-pulse ultrafast optical switching of an elementary ferromagnet. *Commun. Phys.* **5**, 16. https://doi.org/10.1038/s42005-021-00798-8 (2022).
11. Manz, S. *et al.* Reversible optical switching of antiferromagnetism in $TbMnO_3$. *Nat. Photonics* **10**, 653–656. https://doi.org/10.1038/nphoton.2016.146 (2016).
12. Dannegger, T. *et al.* Ultrafast coherent all-optical switching of an antiferromagnet with the inverse faraday effect. *Phys. Rev. B* **104**, L060413. https://doi.org/10.1103/PhysRevB.104.L060413 (2021).

13. Stanciu, C. D. *et al.* All-optical magnetic recording with circularly polarized light. *Phys. Rev. Lett.* **99**, 047601. https://doi.org/10.1103/PhysRevLett.99.047601 (2007).
14. Radu, I. *et al.* Transient ferromagnetic-like state mediating ultrafast reversal of antiferromagnetically coupled spins. *Nature* **472**, 205–208. https://doi.org/10.1038/nature09901 (2011).
15. Ostler, T. A. *et al.* Ultrafast heating as a sufficient stimulus for magnetization reversal in a ferrimagnet. *Nat. Commun.* **3**, 666. https://doi.org/10.1038/ncomms1666 (2012).
16. Wienholdt, S., Hinzke, D., Carva, K., Oppeneer, P. M. & Nowak, U. Orbital-resolved spin model for thermal magnetization switching in rare-earth-based ferrimagnets. *Phys. Rev. B* **88**, 020406. https://doi.org/10.1103/PhysRevB.88.020406 (2013).
17. Graves, C. E. *et al.* Nanoscale spin reversal by non-local angular momentum transfer following ultrafast laser excitation in ferrimagnetic GdFeCo. *Nat. Mater.* **12**, 293–298. https://doi.org/10.1038/nmat3597 (2013).
18. Avilés-Félix, L. *et al.* Single-shot all-optical switching of magnetization in Tb/Co multilayer-based electrodes. *Sci. Rep.* **10**, 5211. https://doi.org/10.1038/s41598-020-62104-w (2020).
19. Ciuciulkaite, A. *et al.* Magnetic and all-optical switching properties of amorphous Tb_xCo_{100-x} alloys. *Phys. Rev. Mater.* **4**, 104418. https://doi.org/10.1103/PhysRevMaterials.4.104418 (2020).
20. van Hees, Y. L. W., van de Meugheuvel, P., Koopmans, B. & Lavrijsen, R. Deterministic all-optical magnetization writing facilitated by non-local transfer of spin angular momentum. *Nat. Commun.* **11**, 3835. https://doi.org/10.1038/s41467-020-17676-6 (2020).
21. Davies, C. S. *et al.* Exchange-driven all-optical magnetic switching in compensated 3*d* ferrimagnets. *Phys. Rev. Res.* **2**, 032044. https://doi.org/10.1103/PhysRevResearch.2.032044 (2020).
22. Tanaka, F., Tanaka, S. & Imamura, N. Magneto-optical recording characteristics of TbFeCo media by magnetic field modulation method. *Jpn. J. Appl. Phys.* **26**, 231–235. https://doi.org/10.1143/jjap.26.231 (1987).
23. Hansen, P., Clausen, C., Much, G., Rosenkranz, M. & Witter, K. Magnetic and magneto-optical properties of rare-earth transition-metal alloys containing Gd, Tb, Fe, Co. *J. Appl. Phys.* **66**, 756–767. https://doi.org/10.1063/1.343551 (1989).
24. Dirks, A. & Leamy, H. Columnar microstructure in vapor-deposited thin films. *Thin Solid Films* **47**, 219–233. https://doi.org/10.1016/0040-6090(77)90037-2 (1977).
25. Harris, V. G., Aylesworth, K. D., Das, B. N., Elam, W. T. & Koon, N. C. Structural origins of magnetic anisotropy in sputtered amorphous Tb-Fe films. *Phys. Rev. Lett.* **69**, 1939–1942. https://doi.org/10.1103/PhysRevLett.69.1939 (1992).
26. Kim, K.-J. *et al.* Fast domain wall motion in the vicinity of the angular momentum compensation temperature of ferrimagnets. *Nat. Mater.* **16**, 1187–1192. https://doi.org/10.1038/nmat4990 (2017).
27. Caretta, L. *et al.* Fast current-driven domain walls and small skyrmions in a compensated ferrimagnet. *Nat. Nanotechnol.* **13**, 1154–1160. https://doi.org/10.1038/s41565-018-0255-3 (2018).
28. Ding, M. & Poon, S. J. Tunable perpendicular magnetic anisotropy in GdFeCo amorphous films. *J. Magn. Magn. Mater.* **339**, 51–55. https://doi.org/10.1016/j.jmmm.2013.03.007 (2013).
29. Lee, J. C. T. *et al.* Synthesizing skyrmion bound pairs in Fe-Gd thin films. *Appl. Phys. Lett.* **109**, 022402. https://doi.org/10.1063/1.4955462 (2016).
30. Woo, S. *et al.* Current-driven dynamics and inhibition of the skyrmion hall effect of ferrimagnetic skyrmions in GdFeCo films. *Nat. Commun.* **9**, 959. https://doi.org/10.1038/s41467-018-03378-7 (2018).
31. Quessab, Y. *et al.* Tuning interfacial Dzyaloshinskii-Moriya interactions in thin amorphous ferrimagnetic alloys. *Sci. Rep.* **10**, 7447. https://doi.org/10.1038/s41598-020-64427-0 (2020).
32. Atxitia, U., Nieves, P. & Chubykalo-Fesenko, O. Landau-Lifshitz-Bloch equation for ferrimagnetic materials. *Phys. Rev. B* **86**, 104414. https://doi.org/10.1103/PhysRevB.86.104414 (2012).
33. Gridnev, V. N. Ferromagneticlike states and all-optical magnetization switching in ferrimagnets. *Phys. Rev. B* **98**, 014427. https://doi.org/10.1103/PhysRevB.98.014427 (2018).
34. Hebler, B., Hassdenteufel, A., Reinhardt, P., Karl, H. & Albrecht, M. Ferrimagnetic Tb-Fe alloy thin films: Composition and thickness dependence of magnetic properties and all-optical switching. *Front. Mater.*https://doi.org/10.3389/fmats.2016.00008 *(2016).*
35. Ma, C. T., Kirby, B. J., Li, X. & Poon, S. J. Thickness dependence of ferrimagnetic compensation in amorphous rare-earth transition-metal thin films. *Appl. Phys. Lett.* **113**, 172404. https://doi.org/10.1063/1.5050626 (2018).
36. Duine, R. A., Lee, K.-J., Parkin, S. S. P. & Stiles, M. D. Synthetic antiferromagnetic spintronics. *Nat. Phys.* **14**, 217–219. https://doi.org/10.1038/s41567-018-0050-y (2018).
37. Chen, J., Tzou, D. & Beraun, J. A semiclassical two-temperature model for ultrafast laser heating. *Int. J. Heat Mass Transf.* **49**, 307–316. https://doi.org/10.1016/j.ijheatmasstransfer.2005.06.022 (2006).
38. Majchrzak, E. & Dziatkiewicz, J. Analysis of ultrashort laser pulse interactions with metal films using a two-temperature model. *J. Appl. Math. Comput. Mech.* **14**, 31–39. https://doi.org/10.17512/jamcm.2015.2.04 (2015).
39. Dzyaloshinsky, I. A thermodynamic theory of "weak" ferromagnetism of antiferromagnetics. *J. Phys. Chem. Solids* **4**, 241–255. https://doi.org/10.1016/0022-3697(58)90076-3 (1958).
40. Moriya, T. Anisotropic superexchange interaction and weak ferromagnetism. *Phys. Rev.* **120**, 91–98. https://doi.org/10.1103/PhysRev.120.91 (1960).
41. Ma, C. T., Xie, Y., Sheng, H., Ghosh, A. W. & Poon, S. J. Robust formation of ultrasmall room-temperature Neél skyrmions in amorphous ferrimagnets from atomistic simulations. *Sci. Rep.* **9**, 9964. https://doi.org/10.1038/s41598-019-46458-4 (2019).
42. Ostler, T. A. *et al.* Crystallographically amorphous ferrimagnetic alloys: Comparing a localized atomistic spin model with experiments. *Phys. Rev. B* **84**, 024407. https://doi.org/10.1103/PhysRevB.84.024407 (2011).
43. Gilbert, T. A lagrangian formulation of the gyromagnetic equation of the magnetization field. *Phys. Rev.* **100**, 1243 (1955).

Acknowledgements

This work was supported by the DARPA Topological Excitations in Electronics (TEE) program (grant D18AP00009). The content of the information does not necessarily reflect the position or the policy of the Government, and no official endorsement should be inferred. Approved for public release; distribution is unlimited.

Author contributions

C.T.M conceived the simulations and analysed the results, W.Z. and S.J.P contributed to discussions. All authors reviewed the manuscript.

Competing interests

The authors declare no competing interests.

Additional information

Correspondence and requests for materials should be addressed to C.T.M.

Reprints and permissions information is available at www.nature.com/reprints.